Published in final edited form as:
Cytometry B Clin Cytom. 2013 November ; 84(6): . doi:10.1002/cyto.b.21088.

Imaging Flow Cytometry for Morphologic and Phenotypic Characterization of Rare Circulating Endothelial Cells:

Samsel; Imaging Flow Cytometry of CECs

Leigh Samsel, MS, **Pradeep K. Dagur, Ph.D.**, **Nalini Raghavachari, Ph.D.**, **Catherine Seamon, BSN**, **Gregory J. Kato, MD**, and **J Philip McCoy Jr., Ph.D.**

[1]Flow Cytometry Core Facility, National Heart Lung and Blood Institute, NIH, Bethesda, MD

[2]Genomics Core Facility, National Heart Lung and Blood Institute, NIH, Bethesda, MD

[3] Cardiovascular and Pulmonary Branch, National Heart Lung and Blood Institute, NIH, Bethesda, MD

Abstract

Endothelial cells in the peripheral circulation are rare events that require technically rigorous approaches for detection by flow cytometry. Visualization of these cells has been even more demanding, as this has historically required extensive enrichment and processing prior to attempting imaging. As a result, few, if any, examples exist of images of peripheral blood CECs that include verification of the cell lineage both phenotypically and genomically. In the present study, we have devised a method whereby CECs can be directly visualized after lysis of red blood cells and staining, without pre-enrichment or additional processing. Peripheral blood is stained with CD45, CD146, CD3, Hoechst, and dapi to permit identification of CD146 positive, non-leukocyte, nucleated and live cells that fit the description of CECs. These cells are imaged using the Amnis Imagestream^X, an imaging flow cytometer. Genomic verification of the endothelial nature of these cells is accomplished by using an aliquot of the same stained samples for sorting CECs using similar gating strategies. This proof of principle of direct imaging of CECs by imaging flow cytometry (IFC) will permit studies to be conducted heretofore not possible, as the Imagestream^X has the capability of detecting additional fluorochromes other than those used to identify the CECs. Such potential investigations include antigen colocalization or capping, autophagy and apoptosis, morphologic changes in response to therapy, as well as many others. Thus, this method will enable a broad range of novel studies to be conducted using CECs as surrogates of the endothelium.

Keywords

Circulating endothelial cells (CECs); Imaging cytometry; Rare event cytometry

Introduction

Circulating endothelial cells (CECs) are angiogenic cells that are extremely rare in normal human peripheral blood (approximately 1-10 per ml of blood)[1,2] and appear in increased numbers in the peripheral circulation as a result of vascular injury or in response to

J Philip McCoy, Jr., 10 Center Drive, Room 8C103D, Bethesda, MD, 20892. Fax: 301-480-4774, Phone 301-451-8824, mccoyjp@mail.nih.gov.

Disclosures
None.

vasculogenic stimuli. CECs have been reported to be present in elevated levels in various disease states[1,2], including patients with sickle cell anemia, indicating their importance as a potential biomarker of disease and indicator of disease state[2]. Various technologies have been used to detect CECs such as traditional flow cytometry, microscopy, or immuno-magnetic bead selection followed by microscopy[2,3]. While these methods permit detection and enumeration of CECs, characterization of these cells has been hampered by the limited number of CECs in the circulation and by the lengthy and labor intensive methods required to isolate these cells for further characterization. For these reasons, imaging of CECs has proven difficult, albeit not entirely impossible. A few reports have offered images of circulating endothelial cells, but these generally suffer from poor morphology and limited number of cells imaged (often a single cell) ([3,4,5]). All of these attempts to image CECs have required two platforms: either flow cytometry or magnetic bead sorting to isolate the CECs followed by fluorescence microscopy on cells layered onto to a slide or coverslip. Further, in none of these instances was there an attempt to verify the endothelial nature of the cells isolated through the use of genomics.

Multi-color flow cytometry, being high throughput and high content, is ideal for rapid analysis of tens of thousands of cells per second to identify rare cells with high specificity and statistical rigor. For this reason, flow cytometry is most often used to quantify CECs. However, the information provided by such immunophenotyping is limited. It provides no information on the morphological or spatial characteristics of cellular markers. For such data, it is necessary to isolate CECs by cell sorting and perform second tier assays. This is both laborious and challenging due to possible cell loss or damage during the isolation process. Microscopy based methods, while enabling morphological and spatial analysis of cells such as CECs and their contents, are further limited by the time required to analyze a statistically significant number of cells, the inability to use a sufficient number of markers to identify the cell of interest, the presence of clumps of cells that make it difficult to discern the morphology of a single cell, and the subjective selection of cells for analysis. These issues render microscopy to limited value for rare event analysis. Imaging flow cytometry (IFC) using the Amnis Imagestream^{X}, combines many features of traditional flow cytometry with microscopy, providing streamlined, multiparameter detection and characterization of the biological properties of large numbers of single cells, thus providing statistical power and specificity for morphological analysis not previously obtainable for rare event analysis[6].

Herein, we describe the novel detection and visualization of CECs from peripheral blood by IFC on the Amnis ImageStream^{X}. The emphasis of this study was visualization and characterization of CECs, rather than the enumeration of these cells, and no attempt was made to perform the latter. This is performed without pre-enrichment by cell sorting or magnetic bead separation followed by subsequent staining and labor intensive microscopy steps. Furthermore, this IFC uses the identical markers as in traditional flow cytometry to assure specific identification of CECs and similar gating strategies as traditional cytometry, consistent with our previous work[1] and only slightly modified from the recommendations of Mancuso et al[7]. This harmonization thereby allows the morphological characterization of live, nucleated single cells by IFC. We have validated that the cells characterized by IFC were in fact CECs, by sorting in parallel an aliquot from the same stained sample on the same day, using near identical gating strategies, for Q-RTPCR analysis for endothelial genes. This study serves as a proof of principle for this methodology and thus will permit new studies of CECs that could include examination of morphology, and spatial distribution of cellular markers in additional to standard phenotypic analyses.

Methods

Preparation of sample for immunophenotyping

Patients with sickle cell anemia were used as donors in this study, as their CEC levels have been reported to be elevated[2]. Figure 1 illustrates how a sample was aliquoted and subsequently processed for either imaging flow cytometry (right column) or for sorting followed by Q-RTPCR (left column) after staining. Approximately 8ml of peripheral blood from sickle cell anemia patients was collected in each of three vacutainer tubes containing ACD Solution A (BD Biosciences, San Jose, CA) for a total of approximately 24mls of peripheral blood. The blood was centrifuged in the original vacutainer tubes for 10 minutes at 400 × g, and the top plasma layer was removed and discarded. The remaining blood in each vacutainer tube was transferred to a 50ml conical tube and diluted 1:10 with ACK Lysing Buffer (Quality Biological, Inc, Gaithersburg, MD). The blood was lysed for 10 minutes at room temperature with gentle rocking. The lysed blood was centrifuged for 10 minutes at 400 × g, the supernatant was discarded, and the cell pellet was resuspended in 5ml ACK Lysing Buffer. The cells were pooled into one 50ml conical tube and were lysed a second time for 10 minutes at room temperature with gentle rocking. The cells were centrifuged for 10 minutes at 400 × g, and the supernatant was discarded. The cell pellet was resuspended in 25 ml FACS Buffer (containing PBS pH 7.2 with 0.5mM EDTA and 0.2% BSA) to wash the cells, centrifuged for 10 minutes at 400 × g, and the supernatant was discarded. The cell pellet was resuspended in 800ul FACS Buffer. 200ul normal mouse serum (Sigma Aldrich, St. Louis, MO) was added and allowed to incubate for 10 minutes at room temperature. A cell count was performed. Cells were reacted with CD146 PE (clone P1H12, BD Pharmingen, San Jose, CA), CD3 AlexaFluor 647 (clone UCHT1, BD Pharmingen, San Jose, CA), and CD45 APC-Cy7 (clone 2D1, BD Pharmingen, San Jose, CA) at room temperature for 30 minutes. As an N-1 control (-CD146 PE), cells were incubated with CD3 and CD45 but not CD146. To sort B cells as a control for subsequent Q-RTPCR, aliquots of the blood were stained with CD20 FITC (clone 2H7, BD Biosciences), CD3 AF647, and CD45 APC-Cy7. After staining, cells were washed with FACS Buffer, resuspended in FACS Buffer to 20×10^6 cells/ml, and incubated with Hoechst 33342 (Invitrogen, Carlsbad, CA) at a final concentration of 0.5uM per million cells at 37° C for 30 minutes. 1.5 μl 7AAD (Beckman Coulter, Carlsbad, CA) was added per million cells. As shown in Figure 1, one aliquot was used for cell sorting (left panel) and one aliquot was used for imaging flow cytometry (right panel). Pooled human umbilical vascular endothelial cells (HUVECs) were procured from Lonza Inc, Rockland, MD and were maintained at 50 to 70% confluence in T-75 flasks in EGM-2 medium supplemented with Bullet kit (Lonza Inc, Rockland, MD) at 37° C and 5% CO2 in a humidified incubator. HUVECs were not reacted with any antibodies and were sorted to use as a control for subsequent Q-RTPCR. Cells were filtered through a 40 micron nylon cell strainer (BD Biosciences, Bedford, MA) before acquisition on cytometers. Patients in this study gave informed consent and the procedures followed were in accordance with institutional guidelines under IRB protocol 03-CC-0015 and this study was performed between November, 2009 and June, 2012.

Imaging Flow Cytometry

Cells for imaging flow cytometry were diluted to a concentration of 5×10^6 cells in 60ul FACS Buffer. Images were acquired on a 2 camera, 12 channel ImageStream^X (Amnis Corporation, Seattle, WA) utilizing 405, 488658, and 785nm lasers, 60X magnification, using Amnis' INSPIRE data acquisition software. Brightfield was collected in Channels 1 and 9 at an intensity of 800, SSC was collected in Channel 6 at a 785nm power of ~2mW, Hoechst was detected in Channel 7 (430-505nm filter) at a 405nm laser power of 10mW, PE and 7AAD were detected in Channels 3 (560-595nm filter) and 5 (660-745nm filter),

respectively, at a 488nm laser power of 200mW, and AlexaFluor 647 and APC-Cy7 were detected in channels 11 (660-745nm filter) and 12 (745-800nm filter), respectively, at a 658nm laser power of 120mW. 60μl of sample was loaded, and 10,000 events meeting the cell classifier were acquired per file at 60X magnification and a 6 micron core diameter. Cell classifiers were set for channel 1 area lower limit of 25 to eliminate collection of debris, channel 3 raw max pixel lower limit of 20 (non-background subtracted pixel intensity of the PE channel) such that the majority of CD146 PE negative events were not collected, and a raw max pixel upper limit of 4094 for all channels used so that events containing saturating fluorescence were not collected. Multiple ~10,000 event files were collected and each file was individually analyzed. For display purposes, files containing CECs were merged to represent one file of ~180,000 events. Compensation and data analyses were performed in IDEAS 4.0 or 5.0 software (Amnis Corporation, Seattle, WA). A compensation matrix was created in IDEAS, utilizing single color controls acquired with the Brightfield and the 785 laser turned off, and all others laser powers set to the powers listed above. A hierarchical gating strategy was created in IDEAS to identify CECs (figure 2). A Brightfield Area versus Intensity_Side Scatter plot was used to identify and gate on low side scatter mononuclear cells. Nucleated (Hoechst+) cells were gated on an Intensity_Hoechst versus Intensity_Side Scatter plot. Live (7AAD negative), nucleated, cells were gated on an Intensity_7AAD versus Intensity_Side Scatter plot. Doublets were eliminated by gating on single cells using an Intensity_CD45 APC-Cy7 versus Aspect Ratio_Brightfield plot. Single, round cells have a higher aspect ratio while elongated cells, aggregates, or more than one cell in a frame have a lower aspect ratio. Live, nucleated, single cells were then plotted on an Intensity_CD3 AlexaFluor 647 versus Intensity_Side Scatter plot and CD3- cells were gated. Live, nucleated, single CD3- cells were plotted on an Intensity_CD45 APC-Cy7 versus Intensity_CD146 PE plot and CECs were gated as CD146+ CD45-. The final CEC gate was set based on the N-1 (-CD146 PE) control, which was used to assess background and non-specific events, and minimize those background events from the CD146+ CD45- CEC gate.

Cell sorting

Cells were sorted on a MoFlo Legacy (Beckman Coulter, Hialeah, FL) and data collected and analyzed using Summit version 4.0. A 488nm excitation wavelength was used for FITC, PE and 7AAD with 530/40, 580/30 and 670/20 collection filters, respectively. A 360nm excitation wavelength was used for Hoechst with a 450/65 collection filter. A 633nm excitation wavelength was used for AlexaFluor 647 and APC-Cy7 with 670/40 and 740LP collection filters used, respectively. Single color controls and unstained cells were run to set compensation. A hierarchical gating strategy was created in Summit to identify CECS (figure 3). A Forward Scatter versus Side Scatter plot was used to identify and gate on low side scatter mononuclear cells. Hoechst+ (nucleated) cells were gated on a Hoechst versus Side Scatter plot. 7AAD negative (live), nucleated, cells were gated on a 7AAD versus Side Scatter plot. A tight gate was created on a Time versus Side Scatter plot to eliminate events caused by perturbations in the stream. Doublets were eliminated by gating on single cells using CD45 APC-Cy7 versus Forward Scatter Pulse Width plot. Live, nucleated, single cells were then plotted on a CD3 AlexaFluor 647 versus Side Scatter plot and CD3- cells were gated. Live, nucleated, single CD3- cells were plotted on a CD45 APC-Cy7 versus CD146 PE plot and CECs were gated as CD146+ CD45-. The final CEC gate was set based on a 1×10^6 event file of the N-1 (-CD146 PE) control, which was used to assess background and non-specific events, and minimize those background events from being included in the CD146+ CD45- CEC gate. CD146+ CD45-, CD3-, live, nucleated, single cells falling within a tight time versus side scatter gate were sorted into 50μl RNA Lysis Solution (Ambion, Austin, TX). The number of CECs sorted depended on the patient and whether or not they were in a sickle cell crisis, but, on average, was approximately 435 CECs. For B and T cell controls, a similar gating strategy was used except for B cells CD20+ CD45+ CD3- cells

were sorted, and for T cells, CD146- CD45+ CD3+ cells were sorted. For sorting HUVECs, a Forward versus Side Scatter plot was set around the main HUVEC population to eliminate debris, and a Pulse Width gate was used to eliminate doublets. 500 B, T, and HUVEC cells were sorted into 50μl RNA Lysis Solution.

Gene expression

Q-RTPCR was performed on the sorted CECs to quantify mRNA encoding MCAM (CD146), Caveolin-1 (CD36), CD34, and von-Willebrand factor (vWF) – all known to be expressed on endothelial cells [2,8,9]. CECs were also screened by Q-RTPCR for the leukocytic markers CD2, CD3e, CD19, and CD20, which should not be expressed on CECs and therefore served as controls. Total RNA from sorted CECs, T-cells, B-cells, and HUVECs was extracted using RNAqueous micro kit (Ambion, Austin, TX) as per the manufacturer's instructions. First strand cDNA synthesis was performed using Superscript cDNA synthesis kit (Invitrogen, Carlsbad, CA) as per the manufacturer's instructions. cDNA was preamplified using pool of Taqman gene expression assays using Taqman PreAmp master mix (Applied Biosystems, Foster City, CA) as per the manufacturer's instructions. This amplified cDNA served as the template for the amplification of gene of interest and the housekeeping genes (GAPDH#Hs02786624_g1) by real time PCR in a 7900-sequence detector (PE Applied Biosystems, Norwalk, CT). In brief, PCR amplifications were performed in a 384 well plate with 20μl volume reaction mixture containing 3.0E-7 mol/L (300nM) of each primer, 2.0E-7 mol/L (200nM) probe, 2.0E-7 (200nM) dNTP in 1X Taqman real time PCR buffer and passive reference (ROX) fluorochrome. The thermal cycling conditions were 2 min at 50°C and 10 min at 95°C, followed by 40 cycles of 15sec denaturation at 95°C and 1 min annealing and extension at 60°C. Samples were analyzed in duplicate and after normalizing the Ct values to the house-keeping gene GapDH, fold changes in expression were calculated using ΔΔCt (cycle threshold) method as shown by Livak and Schmittgen[10]. The primers obtained from Applied Biosystems are as follows: MCAM/CD146 #Hs00174838_m1, Cav-1#Hs00184697_m1, CD34#Hs00990732_m1, PECAM#Hs00169777_ml, vWF#Hs00169795_ml, CD2#Hs01040180_ml, CD3 #Hs01068717_m1, CD19#Hs01047417_g1, and CD20#Hs00544819_ml.

Results

Detection and Imaging of Circulating Endothelial Cells by IFC

One aliquot of the stained cells was imaged on the Amnis ImageStream^X and putative CECs were identified (figure 1, right column). CECs were identified as being single, nucleated, live, CD146+, CD3-, and CD45- cells utilizing the gating scheme shown in Figure 2. A single raw image file (.rif) data file from the Imagestream^X containing sufficient events for detection and analysis of CECs would need to contain several million events and would be several hundreds of gigabytes. The analyses of files of such size are not possible using standard desktop computers (e.g dual quad core, 64 bit systems) with any reasonable speed. It was therefore necessary to acquire Imagestream^X data in a different manner than is usually done for flow cytometry. First, to minimize file size, data were collected using a cell classifier (live event gate) so that the majority of CD146 PE- events were not collected, thus greatly enriching for CD146+ events. This was done for 2 reasons: first, all CECs are identified as CD146+, but only a small percentage (2-3%) of other mononuclear cells express this marker. This permits the collection of files significantly enriched for CECs without inadvertently eliminating some. Second, as this cell classifier gating must be performed during acquisition, and because it is not possible to set compensation during acquisition on the Imagestream^X, the initial .rifs contained true PE+ events and events that came from cells stained with other fluorochromes which bled into the PE channel. Using this

approach, a .rif data file containing 10,000 events could be collected, having a file size of roughly 1- 4gb. Even using this cell classifier (live gate approach), it was necessary to collect multiple 10K .rif files in order to analyze the entire aliquot of any given sample. Each .rif was then analyzed individually using the gating strategy as described above to identify CECs (Figure 2).

Figure 4 demonstrates the necessity of the sequential gating strategy by displaying imagery of cells *not* meeting the gating criteria for each sequential gate (gated out of the analysis). The top panel illustrates how events may be CD146+ but may not be cells with intact nuclei or may be binding CD146 non-specifically, confirming the necessity of a nuclear dye in the analysis. The “Nucleated” gate designates Hoechst+ (nucleated) events to be included in downstream analysis, while the red box denotes anuclear cells gated out of the analysis, with corresponding imagery on the right. The second panel down shows that events may be CD146+ but are dead. Dead cells are known to have the potential to non-specifically bind antibody and it is therefore important to eliminate them from the analysis. The “Live” gate designates 7AAD- (live) events to be included in the downstream analysis, while the red box denotes dead cells gated out of the analysis, with corresponding imagery. The third panel down shows how events in imaging cytometry or traditional flow cytometry may be counted as one event, but may in fact be two cells stuck together, thus the importance of a pulse width parameter in traditional flow cytometry or area versus aspect ratio in IDEAS to eliminate aggregates from analysis. One would not want to include in the analysis information from a non-CEC event. The “Single” gate designates (single/aspect ratio high) events to be included in the downstream analysis, while the red box denotes doublets or aggregates gated out of the analysis, with corresponding imagery. The fourth panel down shows CD146+ T cells, demonstrating the necessity of using a leukocyte marker to eliminate leukocytes from downstream analysis. The “CD3 Neg” gates designates events to be included in the downstream analysis, while the red box denotes CD3+ leukocytes gated out of the analysis, with corresponding imagery. This also shows how IFC allows study of multiple subsets of cells, as one could study the CD146+ T cells independently from CECS in this study.

Figure 5 shows the final step in the sequential CEC gating strategy. The “CEC” gate designates CD146+ CD45- events meeting the sequential CEC gating criteria, and corresponding imagery shows single, live, CD146+ CD45- CECs with clear cellular morphology, intact nuclei, and a distinct but diffuse CD146 staining pattern. Enlarged imagery of CD146+ Hoechst+ CECs taken from numerous experiments is shown.

Validation of Endothelial Gene Expression by Q-RTPCR

A shortcoming of many studies of CECs by cytometric methods is that there is no validation of the endothelial origin of the cells phenotypically identified as CECs. In order to validate that the images we obtained were CECs, we wanted confirmation of the endothelial nature of these cells using Q-RTPCR. Unfortunately, the Imagestream^X instrument does not sort cells, thus it was not possible to genotype the actual cells imaged. As an alternative, validation that the cells characterized by IFC were in fact CECs was accomplished by sorting CECs from a second aliquot of the same stained sample (figure 1, left column). This was performed using a gating strategy (Figure 3) similar to that used for the IFC (Figure 2). Q-RTPCR was performed on the sorted CECs. To serve as controls for the Q-RTPCR, CD146- CD3+ CD45+ T cells were sorted from the CD146 stained sample used for sorting CECs. Cells from a second aliquot of the same sickle cell patients were stained with CD20, CD45, and CD146, and CD146- CD20+ CD45+ B cells were sorted. Finally, unstained HUVECs were sorted as a control for endothelial cells. Levels of mRNA on the sorted CECs confirm the expression of endothelial genes encoding MCAM (CD146), Caveolin-1 (CD36), CD34, and von-Willebrand factor (vWF)– all known to be expressed on endothelial

cells [2,8,9], but not the expression of leukocytic genes on the CECs (Figure 6A and B). This result is consistent with the endothelial gene expression found on the sorted HUVECs, and the lack of leukocytic genes on HuVECs (Figure 6C and D). Conversely, T and B cells displayed expression of the corresponding T and B cells genes without expression of the endothelial-associated genes (Figure 6 E-H).

IFC and/or Q-RTPCR were performed simultaneously three times on the same stained patient sample, each time revealing that CECs could be imaged in one aliquot and a second aliquot sorted in parallel using nearly identical gating strategies yielding cells with message for endothelial genes but not for T or B cells.

Discussion

Previous studies attempting to image CECs have all suffered from the need to pre-enrich cells prior to imaging. Bull et al.[4] describe isolation of CECs with P1H12 (CD146) antibody and microbeads followed by immunohistochemical staining for von-Willebrand factor and P1H12, and subsequent microscopy. Goon, et al.[3] describe anti-CD146 coated immunomagnetic bead purification followed by Ulex/lectin selection and epifluorescence microscopy of CD146-immunobead rosettes. Rowand et al.[5] describe the CellTracks automated system consisting of anti-CD146 magnetic bead purification followed by staining for CD45, CD105, and nuclei with DAPI. Cells are then transferred to the CellSpotter Analyzer fluorescence microscope which is scanned by a CCD camera. Captured frames are analyzed by software to identify CECs. Limitations to these previous methods include being highly labor intensive, requiring multiple purifications and subsequent staining steps resulting in loss of rare events during processing, biases in manual counting, imagery containing unclear cellular morphology and/or sheets or clumps of cells, lack of specificity, and the failure in any of these studies to validate the endothelial nature of these cells using genomic approaches.

There are many benefits to using the ImageStream^X for the detection of rare events such as CECs. It is the first and only imaging flow cytometer to allow imaging of live cells in suspension. One can obtain population statistics and imagery analysis on tens of thousands of cells, which is not possible with fluorescence microscopy or traditional flow cytometry alone. There are enough fluorescence channels to allow the specificity necessary to identify CECs that is required, while still containing additional channels available for use in further studies using additional markers. Utilizing the cell classifier as a live event gate, one can accomplish live cell imaging of large numbers of rare cells without pre-enrichment or subsequent staining and microscopy steps, providing a streamlined, less laborious, less subjective approach. Additionally, one can use the data acquired to look at other cell subsets in the same data files (such as CD146+ T cells, Figure 4, fourth panel down). Possibly one of the greatest benefits is the ability to visually confirm the identity of a single cell using the imagery obtained, whereas with traditional flow cytometry this is not possible. Further, the imagery obtained in this study is of single intact cells with clear morphology, a great improvement over previously published studies of CEC morphology([3,4,5]).

However, quantification of CECs was not attempted using this IFC approach due to some limitations to the ImageStream^X. The ImageStream^X can image at maximum approximately 1000 cells per second, which is far slower than high throughput cytometers. This is most problematic for rare event analysis where large numbers of cells need to be analyzed to identify a sufficient number of cells of interest. In addition, rare event analysis requires collection of millions of events in a single data file, and this is simply not possible due to the enormous size of the file that would be created. Our approach employed live gating to reduce the number of non-CEC events acquired, as well as collection of numerous 10,000 event files. Of each 60ul aliquot loaded onto the ImageStream^X only ~28ul is available for

acquisition. The entire sample could not be collected due to the manner in which the ImageStream^X flushes and loads samples between collections. If there is more than one cell in a frame, IDEAS software will attempt to separate the cells into separate frames. However, if the cells are too close together for the software to distinguish as separate events, two or more cells may remain together in a frame (Figure 4 3rd panel down), and any Intensity measurements or spatial characterization scores would result in the total values of both cells together, rather than from each individual cell, thus affecting quantification. In addition, images that are on the edge of the field of view are eliminated from the analysis as "clipped images". One could elect to include clipped images in the analysis; however, any Intensity measurements or spatial characterization scores would result in partial values of the clipped image, thus affecting quantification.

In this report, we have shown that images of cells fitting the phenotypic criteria of CECs can be imaged by IFC without the use of any pre-enrichment processes, and have validated the endothelial origin of these cells by concomitant Q-RTPCR. Imaging flow cytometry, unlike previous methods to visualize CECs, permits streamlined identification of single, live CECs with intact nuclei and clear cellular morphology, using sufficient markers to definitively identify CECs. Because the Imagestream is capable of polychromatic cytometry, this technique should be readily adaptable to other approaches for identifying pro-angiogenic cells, such as that described by Pradhan and colleagues (15). Direct imaging of CECs is important in advancing the use of these cells as biomarkers of disease as this permits further studies on CEC characteristics and function that are not currently possible using other techniques. For example, the formation of new capillaries requires cell elongation for the polarization and directed migration of endothelial cells, and cell shape changes in endothelial cells are seen with nuclear shape remodeling, a possible regulator of genome function[11]. These morphological features, if present in CECs, could readily be measured by IFC and thus relate specific functions to these cells. Furthermore, because the ImagestreamX is a 12 channel instrument and we used only 7 channels in this study, 5 channels remain where other markers of interest can be used to further characterize CEC function provided that suitable fluorochromes can be identified. This would permit additional studies such as those for endothelial autophagy or apoptosis, which have been shown to be important in endothelial biology[12, 13]. Other studies could include endothelial activation using a combination of morphology and cell surface markers. Furthermore, much might be learned from the distribution of markers on the surface of CECs. For example, many cell adhesion molecules redistribute during endothelial migration and detecting these redistributions would permit CECs to be classified as either migratory or non-migratory. Yet additional studies could include co-localization of antigens, and antigen capping. Supplemental figures 1 and 2demonstrate preliminary studies of apoptosis and of CD144 antigen co-expression of CECs. None of these applications are practical by traditional flow cytometry on rare CECs, yet are very feasible using IFC on the ImageStream^X. An additional benefit to this technique is the ability to concomitantly study CD146+ T cells, a relatively rare subset of IL-17 secreting effector memory T cells in the peripheral circulation[14] (Figure 4, right, 4th panel down).

In summary, we have demonstrated the feasibility of imaging rare events in the circulation, specifically circulating endothelial cells by imaging flow cytometry without the need for any pre-enrichment processes. This will permit new approaches to evaluating the use of CECs as surrogate markers of the endothelium. Furthermore, a similar approach could be used for direct characterization of other rare cells in the circulation such as circulating tumor cells or hematopoetic stem cells. It should be noted that since the original submission of this manuscript, a new generation of the Imagestream, the ISX-MkII, has been released. Among the many improvements in this latest generation are the ability to perform live compensation

and perform population gating on compensated events. Such features should further facilitate studies such as the present one.

Supplementary Material

Refer to Web version on PubMed Central for supplementary material.

Acknowledgments

We would like to thank Kimberly Woodhouse in the Genomics Core Facility, National Heart Lung and Blood Institute, NIH, Bethesda, MD, for assistance with the Q-RTPCR and Angelique Biancotto, Center for Human Immunology, NIH, Bethesda, MD, for assistance with figures.

Sources of Funding

Funding for this work was provided by the Division of Intramural Research, National Heart Lung and Blood Institute, NIH, Bethesda, MD.

Non-standard Abbreviations and Acronyms

CECs	Circulating Endothelial cells
PE	Phycoerythrin
IFC	Imaging flow cytometry
vWF	von-Willebrand factor
HUVEC	Human umbilical vein endothelial cells

References

1. Khan SS, Solomon MA, McCoy JP Jr. Detection of circulating endothelial cells and endothelial progenitor cells by flow cytometry. Cytometry B Clin Cytom. 2005; 64:1–8. [PubMed: 15668988]
2. Blann AD, Woywodt A, Bertolini F, Bull TM, Buyon JP, Clancy RM, Haubitz M, Hebbel RP, Lip GY, Mancuso P, Sampol J, Solovey A, Dignat-George F. Circulating endothelial cellsS. Biomarker of vascular disease. Thromb Haemost. 2005; 93(2):228–235. [PubMed: 15711737]
3. Goon PK, Boos CJ, Stonelake PS, Blann AD, Lip GY. Detection and quantification of mature circulating endothelial cells using flow cytometry and immunomagnetic beads: a methodological comparison. Thromb Haemost. 2006; 96:45–52. [PubMed: 16807650]
4. Bull TM, Golpon H, Hebbel RP, Solovey A, Cool CD, Tuder RM, Geraci MW, Voelkel NF. Circulating endothelial cells in pulmonary hypertension. Thromb Haemost. 2003; 90:698–703. [PubMed: 14515191]
5. Rowand JL, Martin G, Doyle GV, Miller MC, Pierce MS, Connelly MC, Rao C, Terstappen LW. Endothelial cells in peripheral blood of healthy subjects and patients with metastatic carcinomas. Cytometry A. 2007; 71(2):105–13. [PubMed: 17226859]
6. Basiji DA, Ortyn WE, Liang L, Venkatachalam V, Morrissey P. Cellular image analysis and imaging by flow cytometry. Clin Lab Med. 2007; 3:27, 653–70.
7. Mancuso P, Antoniotti P, Quarna J, Calleri A, Rabascio C, Tacchetti C, Braidotti P, Wu HK, Zurita AJ, Saronni L, Cheng JB, Shalinsky DR, Heymach JV, Bertolini F. Validation of a standardized method for enumerating circulating endothelial cells and progenitors: flow cytometry and molecular and ultrastructural analyses. Clin Cancer Res. 2009; 15(1):267–73. [PubMed: 19118054]
8. Smirnov DA, Foulk BW, Doyle GV, Connelly MC, Terstappen LW, O'Hara SM. Global gene expression profiling of circulating endothelial cells in patients with metastatic carcinomas. Cancer Res. 2006; 66(6):2918–22. [PubMed: 16540638]

9. Rigolin GM, Maffei R, Rizzotto L, Ciccone M, Sofritti O, Daghia G, Cibien F, Cavazzini F, Marasca R, Cuneo A. Circulating endothelial cells in patients with chronic lymphocytic leukemia: clinical-prognostic and biologic significance. Cancer. 2010; 116(8):1926–37. [PubMed: 20166207]

10. Livak KJ, Schmittgen TD. Analysis of relative gene expression data using real-time quantitative PCR and the 2(-Delta Delta C(T)) Method. Methods. 2001; 25(4):402–408. [PubMed: 11846609]

11. Versaevel M, Grevesse T, Gabriele S. Spatial coordination between cell and nuclear shape within micropatterned endothelial cells. Nature Commun. 2012:3–671.

12. Du J, Teng R- J, Guan T, Eis A, Kaul S, Konduri G, Shi Y. Role of autophagy in angiogenesis in aortic endothelial cells. Am J Physiol Cell Physiol. 2012; 2:302, 383–391.

13. Singh N, Van Craeyveld E, Tjwa M, Ciarka A, Emmerechts J, Droogne W, Gordts SC, Carlier V, Jacobs F, Fieuws S, Vanhaecke J, Van Cleemput J, De Geest B. Circulating apoptotic endothelial cells and apoptotic endothelial microparticles independently predict the presence of cardiac allograft vasculopathy. J Am Coll Cardiol. 2012; 4:60, 324–331.

14. Dagur PK, Biancotto A, Wei L, Sen N, Yao M, Strober W, Nussenblatt RB, McCoy JP. MCAM–Expressing CD4+ T Cells in Peripheral Blood Secrete IL17A and are Significantly Elevated in Patients with Inflammatory Autoimmune Diseases. J Autoimmunity. 2011; 37:319–327. [PubMed: 21959269]

15. Pradhan KR, Mund JA, Johnson C, Vik TA, Ingram DA, Case J. Ploychromatic Flow Cytometry Identifies Novel Subsets of Circulating Cells with Angiogenic Potential in Pediatric Solid Tumors. Cytometry Part B. 2011; 80B:335–338.

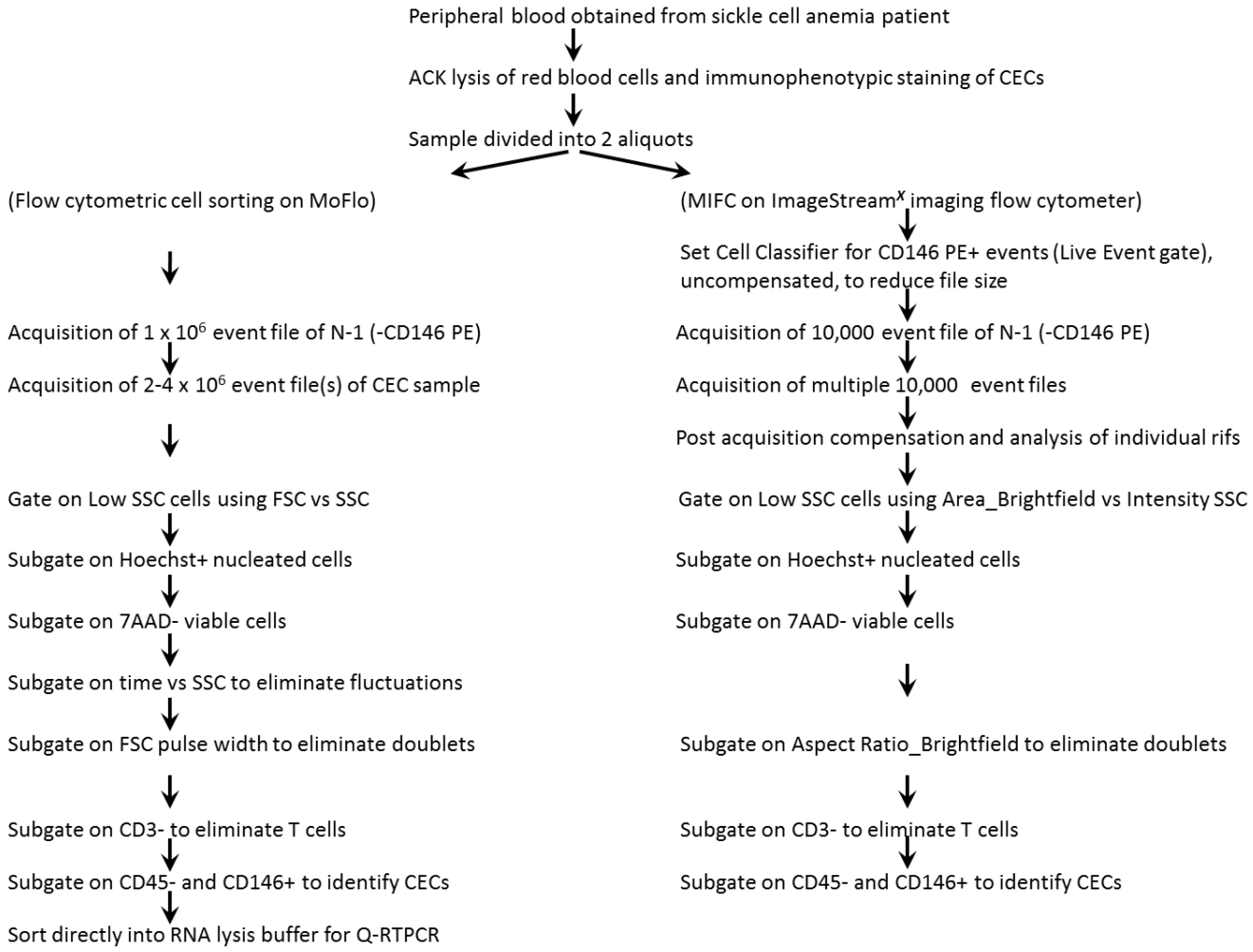

Figure 1.

Flow chart depicting concomitant CEC identification in sorting and IFC platforms. Peripheral blood from sickle cell patients was immunophenotypically stained for CEC identification. The sample was split into two aliquots whereby one was sorted on a MoFlo for Q-RTPCR and confirmation of endothelial gene expression in CECs (left column) and the other was imaged on the ImageStream^X for characterization of CECs (right column). Similarities and differences between the two platforms and their associated gating strategies are evident by comparing the two columns.

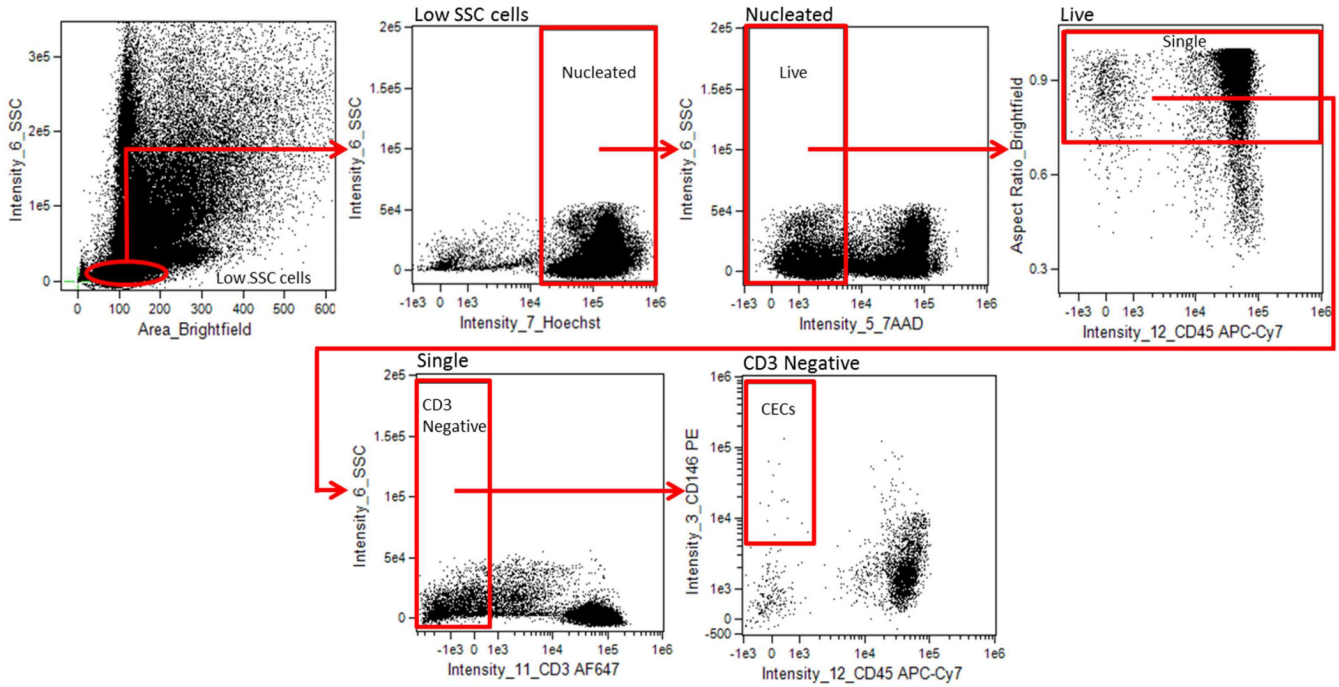

Figure 2.

Gating strategy utilized to identify nucleated, live, single, CD3-, CD45-, CD 146+ CECs on ImageStream^X. For display purposes, 180,000 events are shown from merged files. Low side scatter mononuclear cells were selected using an Area_Brightfield versus Intensity_SSC plot. Nucleated cells were selected as Hoechst+ on an Intensity_Hoechst versus Intensity_SSC plot gated on low side scatter cells. Live cells were selected as 7AAD- on an Intensity_7AAD versus Intensity_SSC plot gated on nucleated cells. Single cells were selected on an Intensity_CD45 versus Aspect Ratio_Brightfield plot gated on live nucleated cells. Rounder objects and single cells have higher aspect ratios. Aggregates, two cells in one frame, or elongated cells have lower aspect ratios (see Figure 4, 3rd panel down). CD3 negative events were selected on an Intensity_CD3 versus Intensity_SSC plot gated on live nucleated single lymphocytes. CD146+CD45- CECs were selected on an Intensity_CD45 versus Intensity_CD146 plot gated on live nucleated single CD3- cells.

Figure 3

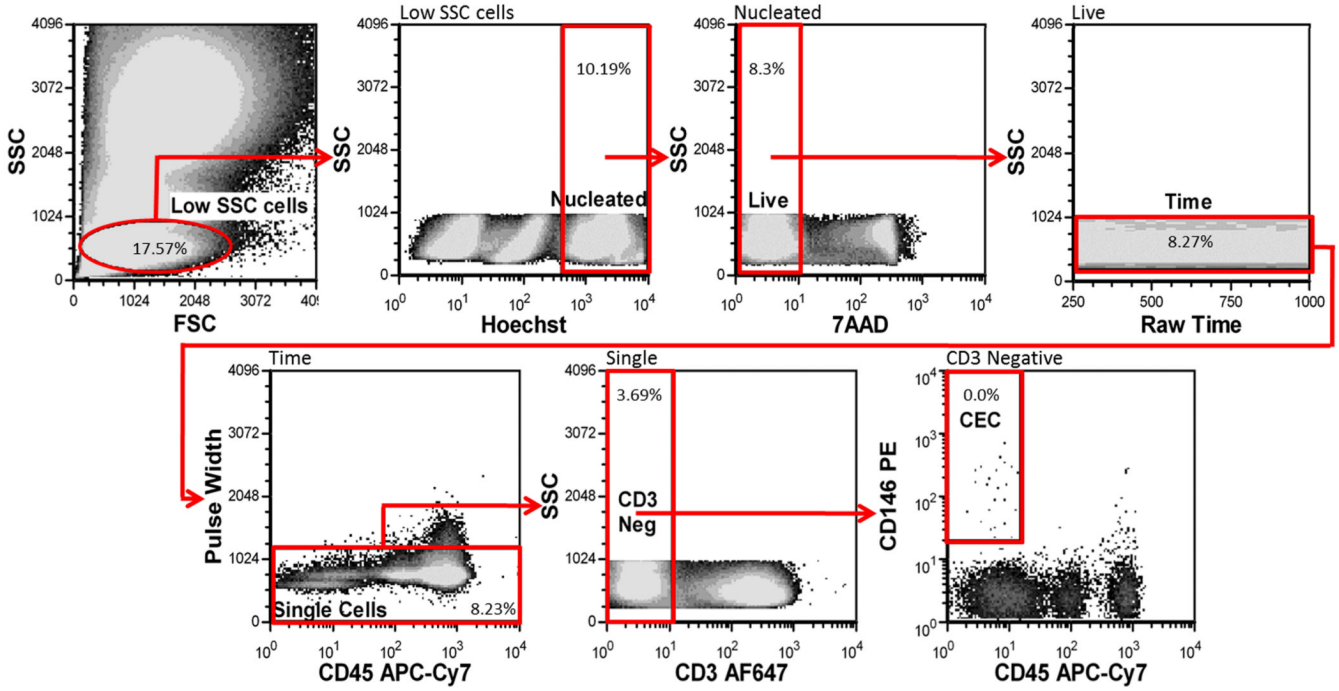

Figure 3.

Gating strategy utilized to identify nucleated, live, single, CD3-, CD45- CD146+ CECs which fall within a tight Time gate on MoFlo. Four million total events are shown. Low side scatter mononuclear cells are identified on a FSC versus SSC plot. Nucleated events are selected as being Hoechst+ on a Hoechst versus SSC plot gated on low side scatter cells. Live cells were selected as being 7AAD- on a 7AAD versus SSC plot gated on nucleated cells. Events arising from a perturbation in fluidics are identified and gated out using a tight gate on a Raw Time versus SSC plot gated on live nucleated cells. Doublets and aggregates were identified and gated out using a CD45 versus Pulse Width plot gated on live nucleated single cells which fall within a tight Time gate. CD3- events are selected on a CD3 versus SSC plot gated on live nucleated single cells which fall within a tight Time gate. Finally, CD146+CD45-CECs are selected on a CD45 versus CD146 plot that is gated on live nucleated single CD3- cells which fall within a tight Time gate.

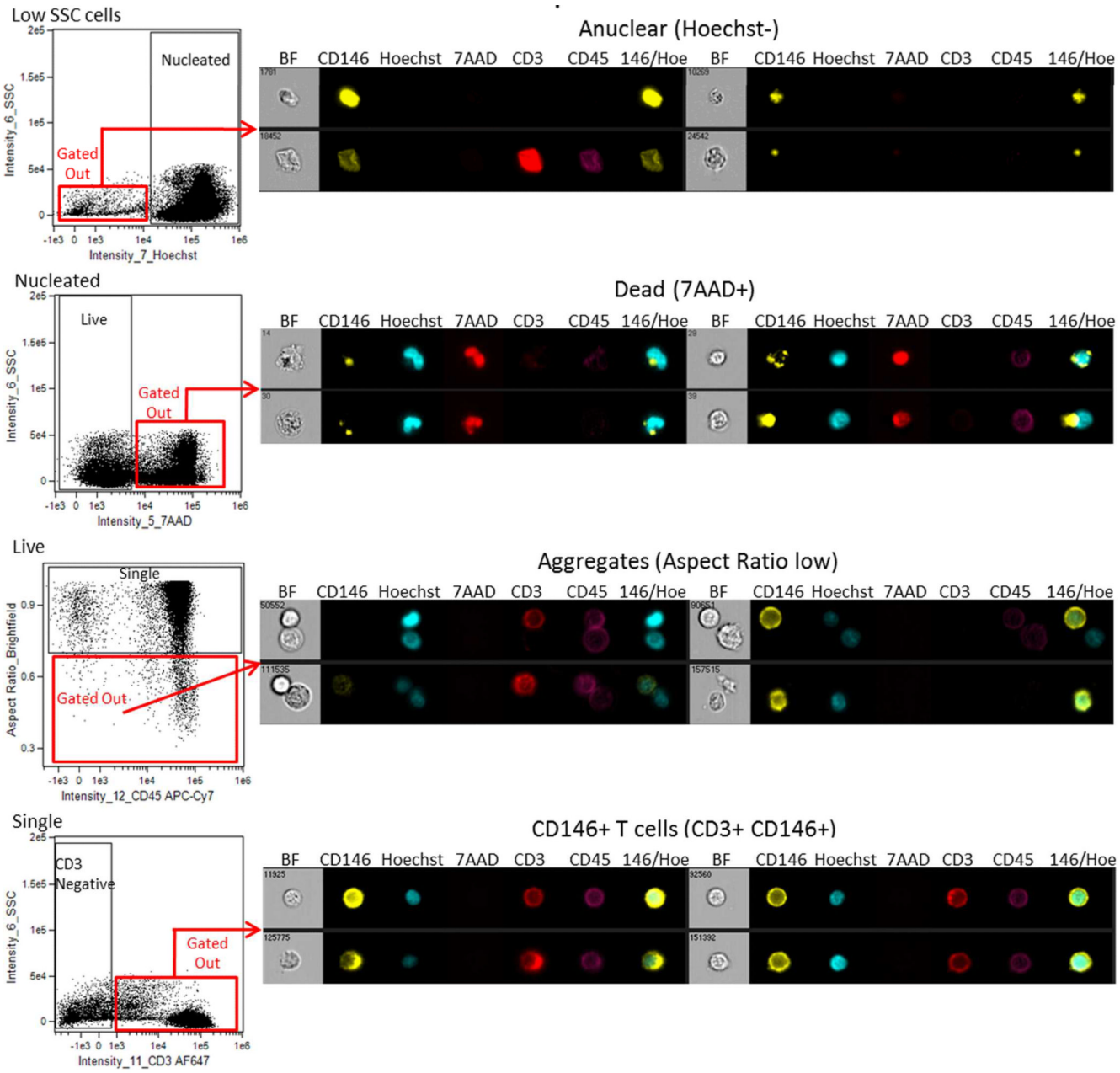

Figure 4.

Representative imagery of cells gated out of the analysis, obtained at 60X magnification on ImageStream^X. To demonstrate the necessity of the sequential gating strategy for flow cytometric detection of CECs described in this manuscript, events ***not*** meeting the CEC gating criteria are shown originating from red boxes, and corresponding imagery is displayed. The top panel shows CD146+ Hoechst- anuclear cells. The second panel shows CD146+ 7AAD+ dead cells. The third panel shows CD146+ and CD146- cells arising from low aspect ratio together in one frame. The fourth panel shows CD146+ CD3+ activated T-cells. For display purposes, intensity of color was adjusted but raw data remained unchanged.

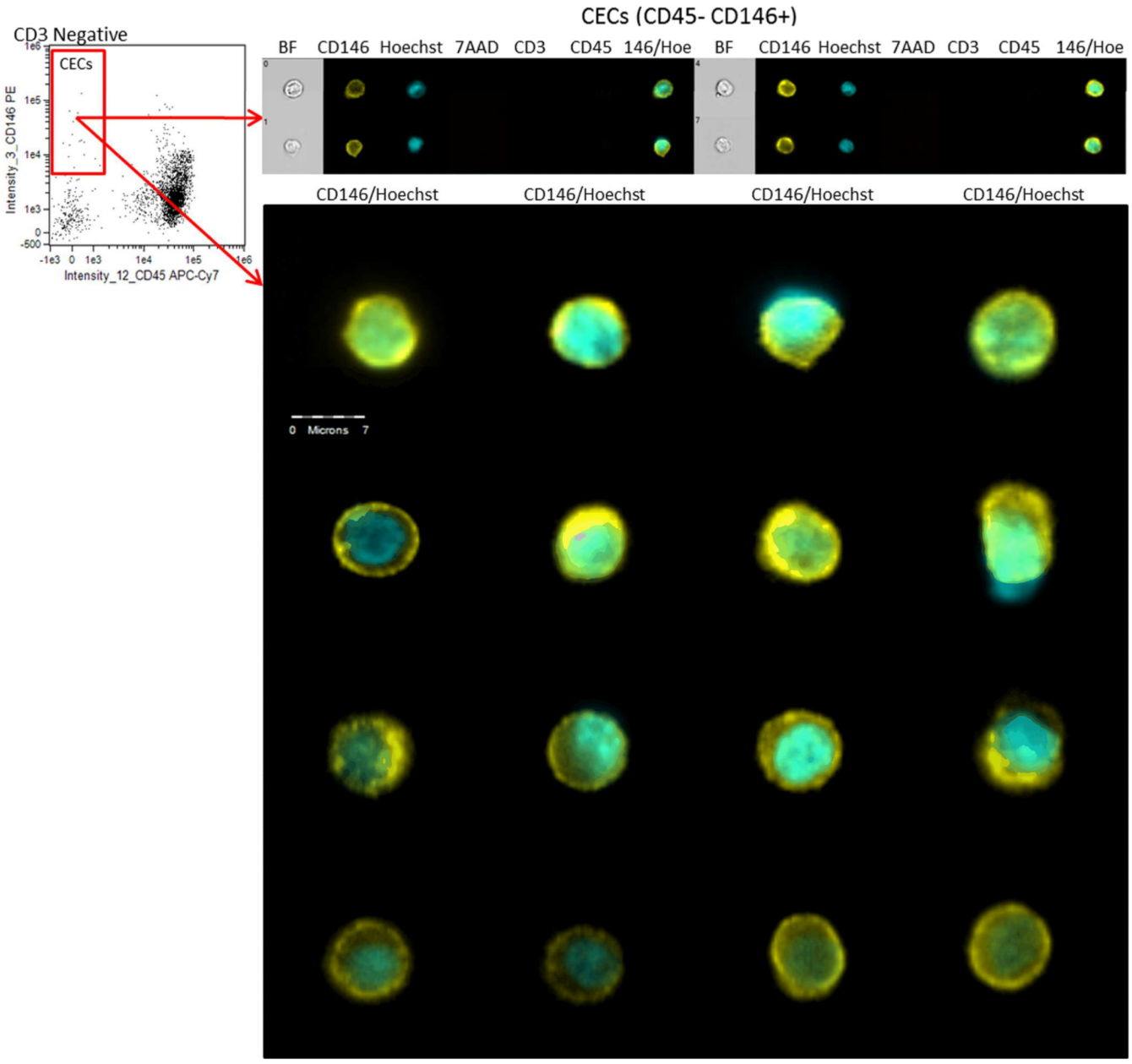

Figure 5.

Representative imagery of CECs obtained at 60X magnification on the ImageStream^X Hoechst+ (nucleated), 7AAD- (live), single (high aspect ratio), CD3- (non-activated T-cells) CD146+CD45- CECs are shown originating from the red box, and corresponding CEC imagery in displayed. The bottom panel shows enlarged imagery of CD146 and nuclear merged images. For display purposes, intensity of color was adjusted but raw data remained unchanged.

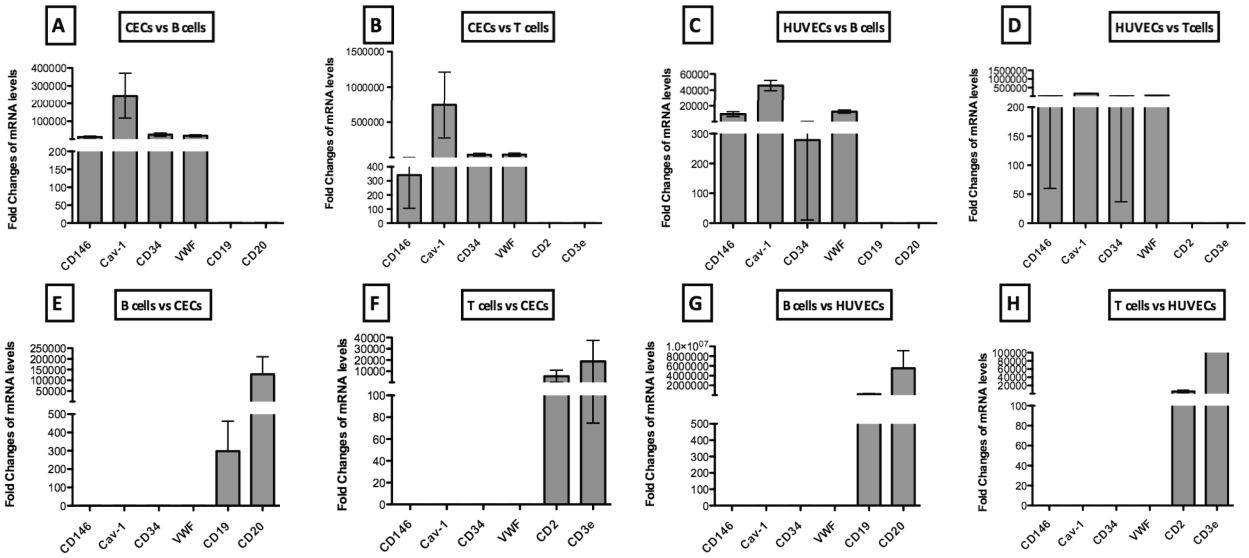

Figure 6.

Fold Changes of relative gene expression resulting from Q-RTPCR on sorted CECs, HUVECs, and T, and B cells. Sorted CECs and HUVECs showed mRNA expression levels consistent with endothelial genes while not showing high levels of leukocytic gene expression, while T and B cell controls showed high mRNA expression levels for corresponding leukocytic genes, but not for endothelial genes. Levels of gene expression are fold changes of A) CECs as compared to B cells B) CECs as compared to T cells C) HUVECs compared to B cells D) HUVECs compared to T cells E) B cells compared to CECs F) T cells compared to CECs G) B cells compared to HUVECs, and H) T cells compared to HUVECs.